4 February 2020
Alessia.Ciccotelli@cern.ch

FLUKA simulations of the operational injection losses in TI8/IR8

A. Ciccotelli, C. Bracco, F. Cerutti, L.S. Esposito, M.A. Fraser, V. Kain, A. Mereghetti, F.M. Velotti
CERN, CH-1211 Geneva, Switzerland

Keywords: Injection, Transfer line, TI8, Beam Loss Monitor, Losses, FLUKA, LIU

Summary

This document describes the FLUKA studies of SPS-to-LHC injection losses. The TI8/IR8 model has been developed especially to understand and predict the effect of the proton impacts on the passive protection system of the SPS-to-LHC transfer line of beam 2. It provides a powerful tool for designing new loss mitigation solutions. The Run-2 commissioning data was instrumental in carrying out a benchmark study and building confidence into the model. The absolute comparison with experimental measurements, including a quench event, provides a better physical understanding of beam loss effects. The High-Luminosity LHC (HL-LHC) upgrade requires substantial changes in the full chain of the LHC injectors. In accordance with LHC Injectors Upgrade (LIU) project, a new transfer line protection system has been designed to attenuate HL-LHC beam to safe levels in case of mis-injection. The TI8 model was used to simulate loss effects in the new layout and to design a dedicated shielding system for the LHC-BLMs.

Contents

1 Introduction

The LIU (LHC Injectors Upgrade) project [1] aims at improving the parameters of the beam injected into LHC: not only the bunch intensity will increase but the transverse emittance will decrease significantly in order to match the HL-LHC requirements. The future HL-LHC beams, with a brightness double of present record, require to upgrade the SPS-to-LHC transfer line collimation and protection systems. The studies of the shower simulations during the beam injection into LHC demand the development of a complex 3D geometry model of the transfer line and LHC beam lines.

The present study intends to investigate the effect of the proton impacts on the passive protection system of the SPS-to-LHC transfer line of beam 2 and related to the beam loss monitor readings. Following the collimator position changes in the upgraded scenario, the TI8 study aims to understand how to shield BLM from regular transfer losses which should not trigger LHC dump. However, the understanding of the losses in the present scenario would provide confidence to the model. The transfer line collimator system (TCDI) protects the transfer line (TL) and especially LHC aperture from damages in case of erroneous transfer [2] [3]. The beam loss monitor (BLM) systems detect beam losses along both the accelerator and the transfer line. During the injection of the beam into LHC, losses at the TCDI might induce signals above the dump threshold in some of the LHC-BLMs close to TI8 collimators. Therefore, those LHC-BLMs might trigger unnecessary beam dump requests in case of injection losses that are not actually unsafe for LHC magnets. As mitigation action, some of the LHC-BLMs placed on the injected beam side (specifically on LHC beam 2 side in case of TI8) are currently filtered during the injection introducing a delay in the acquisition of signals. Another mitigation measure is the installation of dedicate shields that can attenuate the signal of the most exposed LHC-BLMs and, therefore, increase the chance to avoid blinding them during the injection. Previous FLUKA studies of the injection regions led to the design of the present LHC-BLM shields installed along the last part of the transfer lines into the LHC [4] [5] [6].

The present study analyses the beam losses on TCDI and correlates them with induced BLM signals. The validation is based on the comparison between FLUKA simulation predictions of beam loss monitor signals and the measurements performed in a controlled experimental setup. After evaluating the predictive ability of TI8 model in the present LHC layout, a shielding solution has been designed to reduce the LHC-BLM signals induced by injection losses in the future LIU scenario [2].

2 Experimental scenario

The last part of the injector chain into the LHC consists of two transfer lines (TI) steering the beam from the SPS to the LHC rings. The TI2 line injects the beam 1 (B1) into the Insertion Region 2 (IR2) of the LHC towards the Alice experiment, while the TI8 line injects the beam 2 (B2) in the IR8 toward the LHCb experiment.

TI8 is a 3 km long sloping tunnel which starts from the LSS4 of the SPS and ends, after a vertical drop of 70 m, in UJ88 alcove of the LHC. The collimator system is placed in the last part of the tunnel before the injection point into LHC. Lost protons hitting the TCDIs generate particle showers that affects both LHC and SPS-to-LHC transfer line. Beam loss monitor systems are placed along the transfer lines (BLMI) and in LHC ring (LHC-BLM). BLMIs monitor the loss beam during the transfer into the LHC. Injection losses are produced by single beam passage and the BLMI system can only inhibit the next injection in case high losses are detected at the BLMI monitors. However, as mentioned in Sec. 1, those losses along the transfer line might induce high dose values in the LHC-BLMs and trigger an unnecessary beam dump request in case the induced signal is higher than the dump threshold. It is noted that the LHC-BLM dump thresholds are set in relation to possible harmful losses due to the beam circulating in the LHC.

2.1 Transfer line collimator system

The transfer line collimator system consists of TCDI collimators and TCDIM protection masks. The collimators are passive absorber blocks with carbon movable jaws. A set of six TCDIs is placed in each injection line to protect the LHC aperture from particles injected with dangerously large amplitudes. There are three collimators for the horizontal plane (TCDIH) and three for the vertical plane (TCDIV). Each collimator is placed at intervals of 60° betatron phase advance [2]. Moreover, four protection masks (TCDIM) are installed downstream of TCDI collimators. TCDIMs are passive absorber masks protecting local elements from particle showers originated by the protons impinging on the collimator jaws.

Each TCDI is mounted on a specific support designed to satisfy the height of the nominal beam line, the slope and the tilt of the floor. TCDIH motors are placed under the element while the TCDIV ones are side-ward. An alignment system and electrical connectors are installed on the side of all of them. Shower particle interact also with the components of the collimator tank, motors and supports and, therefore, the signal measured by the BLMI closer to the collimator is partially attenuated. In order to estimate the BLM signal accurately, a simplified model of the motors and aluminum support plate was implemented.

The movable jaws are normally centered around the beam path. The aperture, defined as the gap between them, is expressed in units of the local betatronic sigma (σ).

2.2 Beam Loss Monitors

The model includes two types of BLM systems:

1. The BLMI system. These monitors are placed in the injection lines, after each collimator and on sensitive beam-line elements. BLMIs are connected to the Beam Interlock System (BIS) and during the injection, if needed, they can prevent beam permit on the subsequent cycles [7].

2. The LHC-BLM system. Different types of detector are available but, only ionization chambers are considered here. They are positioned on both sides of the LHC: in IR8 of LHC, B2-side BLMs are outside the ring and are closer to TI8 beam pipe. B1-side BLMs are inside the LHC and farther from TI8 collimators and typically shielded from the LHC magnets.

The BLMI system can directly monitor the amount of lost protons on each collimator. Mis-injections can give high signals over the safe threshold of the BLMIs. In addition, the secondary particles generated by the interaction of protons with the collimator jaws induce a signal in the adjacent LHC-BLMs.

The front-end electronics provides 12 output signals (running sums RS) corresponding to as many as integration periods, from 40 μs to 84 s [8].The LHC-BLM signals are expressed in Gy per second (Gy/s). The BLM threshold are set depending on the energy and on loss duration. The saturation level is 23 Gy/s.

Even if the injection losses are single passage losses, the shortest acquisition time (RS 1) does not measure the entire signal because the ion collection time is 85 μs [9]. Figure 1 shows that the experimental dose values are not constant as function of the RS (LHC-BLM signal in Gy/s are multiplied by the corresponding integration period). For B1-side BLM, even without filter, the signal reaches a plateau for $RS \geq 3$, which corresponds to the first RS longer than the ion collection time (see Fig. 1a). As illustrated in Fig. 1b, the effect of the filter is to spread the collected signal of the B2-side BLM over a longer time. For $RS \geq 6$, signals are not affected by the filter effect. The rise in correspondence of the RS 12 signal is due to an average over multiple injections with different oscillation amplitudes (the time interval between two consecutive injections was about 30 seconds). For this study, RS 3 and RS 7 are taken for B1- and B2-side BLMs, respectively.

2.3 Controlled loss scenarios

A major challenge to study the injection loss was to find a well-defined experimental scenario for which a suitable source term can be used as input for the shower simulations. The measurements during the commissioning of the transfer line at the start of the LHC runs are the best reference configurations [10]. The following two scenarios used for the model validation:

1. **BLMI signal calibration**. In this experimental set-up, one collimator jaw is closed to -5 betatronic σ, while the other jaw is fully open. The closed jaw intercepts essentially the whole beam. For the i-th jaw, the calibration factor C_i is defined as:

$$C_i[Gy/p^+{}_{impacting}] = \frac{S_i^{\mathrm{BLMI}}[Gy]}{I[p^+{}_{inj}]} \tag{1}$$

   where S_i^{BLMI} is the BLMI signal and I is extracted protons from SPS which is assumed to be the current at the beginning of simulated TL. Therefore, C_i represents the dose per impacting proton.

   For TI8, the reference calibration factors were measured in 2016 and used for the entire Run-2. It is worth to mention that a variation of about a factor of 2 was measured for the TI2 measurements between 2016 and 2017. This factor should be considered as a systematic error of the measurement.

2. **Loss map method**. Each collimator aperture is fixed at 5 local betatronic σ. Large oscillations of the beam - produced by changing the setting of the kickers at the beginning of the transfer line (TT40) - span different phases and induce losses on few collimators. The BLM signals allow to validate the TCDI set-up [10]. Data collected in 2016, 2017 and 2018 with $5\,\sigma$ amplitude are considered in this study.

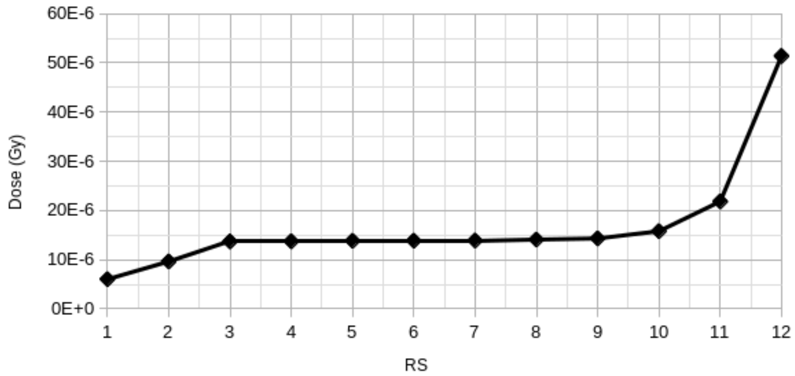

(a) B1-side LHC-BLM without filter

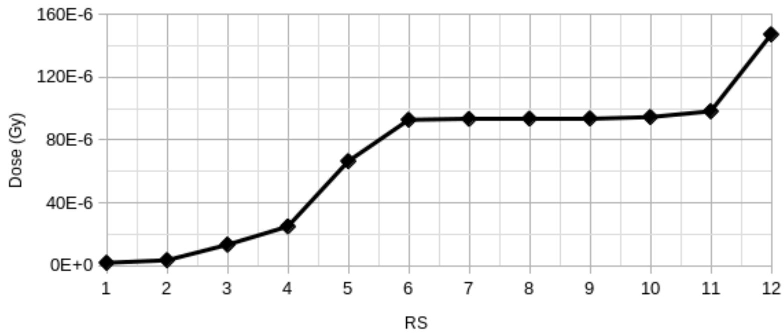

(b) B2-side LHC-BLM with filter

Running sum (RS)	Duration
1	40 μs
2	80 μs
3	320 μs
4	640 μs
5	2.6 ms
6	10 ms
7	82 ms
8	655 ms
9	1.3 s
10	5.2 s
11	21 s
12	84 s

Figure 1: (Top) Example of a signal induced by injection losses on a B1-side LHC-BLM, where the filter is not applied. The slope through RS 1-3 is due to the charge collection time of the monitor. (Bottom) As above but for a B2-side LHC-BLM where the effect of the applied filter is visible and the plateau is reached from RS 6.

3 Simulation model and methods

The study of the injection losses in TI8 required a 3-dimensional model of the last 230 metres of the transfer line. The geometry considered is extensive and includes two different machines, LHC and the SPS-to-LHC injection line (see Fig. 2a and Fig. 2b). FLUKA, a multi-purpose Monte Carlo code, has been used to describe particle interactions in a such complex geometry [11] [12].

In order to implement this geometry, FLUKA Element Database (FeDB) and the Linebuilder (LB) have been used [13]. The FeDB is a database containing the FLUKA geometry models of different accelerator components (magnets, collimators, absorbers, BLMs, etc..), which are used with a modular approach to build the whole geometry. The LB is a Python-based tool for assembling accelerator beam lines for FLUKA simulations (e.g. LHC, SPS, PS). In particular, it allows to arrange accelerator components from FeDB on the basis of TWISS file information. To combine the two machines, the geometry was created with a new two-step procedure:

1. LHC beam line elements were mounted in the 3D tunnel starting from the LHC TWISS file;

2. TI8 beam line elements were mounted in the resulting geometry model of the first step on the basis of TI8 TWISS file.

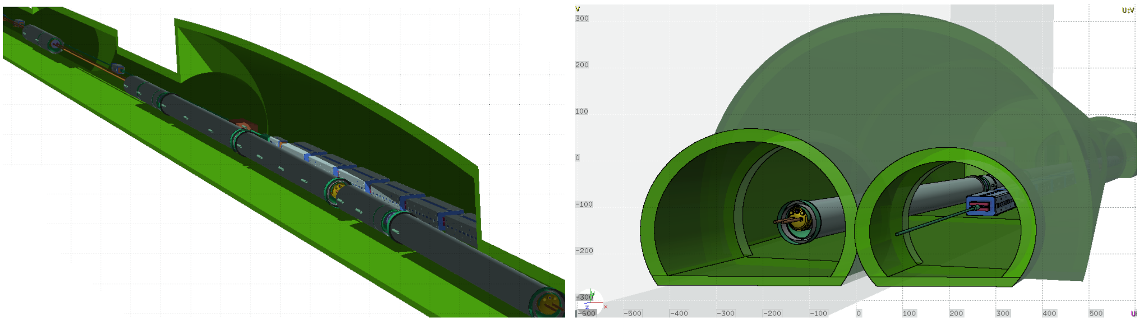

(a) 3D view. (b) 3D cross-section.

Figure 2: TI8 geometry

Figure 3 shows a top view of the geometric model, which includes the LHC cells from Q6 to Q8, the section of the TI8 tunnel and adjacent alcoves. The LHC elements and beam pipes lie on the same level, in the most upstream part of the TI8 tunnel included in the model, the beam pipe is offset by about 5 and 1.4 meters horizontally and vertically, respectively, with respect to the LHC beam line. The TI8 model ends shortly before the injection septum (MSI) where injected beam joins with B2 pipe. An iron shield surrounding the TI8 beam pipe in the UJ87 was already put in place in 2011 to mitigate the effect induced by beam losses during injections into LHC[4].

The magnetic fields in the LHC are not implemented in the model because the effect is considered to be not relevant for this study. The geometrical model does not include jumper

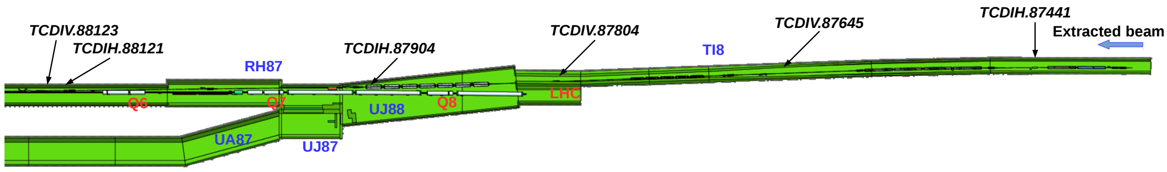

Figure 3: Top view of TI8 model

cables and tanks that should provide a shower attenuation effect. In addition, the TI8 pipe close to the Q6 magnet gets very close to LHC elements and small differences in relative position (both horizontally and vertically) of the BLM monitors might contribute to the simulation inaccuracy.

3.1 MAD-X source input

Different distributions of primary protons impinging on the TCDI collimators are used for the loss studies. The shower induced by the interaction between 450 GeV/c protons and the jaws has been studied. The loss maps are generated by MAD-X. For the simulation of the BLMI signal calibration introduced in section 2.3, the source term is a Gaussian beam travelling on the ideal trajectory sampled from the TWISS parameters. For the study of the beam large oscillations with different phases, the loss maps contain only the protons impacting onto the collimator jaws. The complete distribution at the beginning of the geometry has been used to perform sensitivity analysis to collimator aperture settings [10].

The injected beam trajectory, as simulated in FLUKA, is consistent within an accuracy of $15\,\mu$m with the nominal one, over the considered region.

The beam current was equivalent to pilot intensity ranging from $4 \cdot 10^9$ to $9 \cdot 10^9$ ppp.

4 Validation results

4.1 BLMI signal calibration

This scenario provides the simplest configuration to validate the model. Basically, all beam particles interact with the jaw. The difference in the BLMI signals between a Gaussian beam and a pencil beam was evaluated to be negligible. Since the BLMI signals are very sensitive to their position relatively to the collimator, the actual BLMI positions (not reported in the official documentation) was measured during a site visit of the TI8 tunnel. It was calculated that a displacement of 10 cm in transverse position (distance between BLM and pipe), equivalent to the transverse dimension of the monitor, may lead to a difference of more than

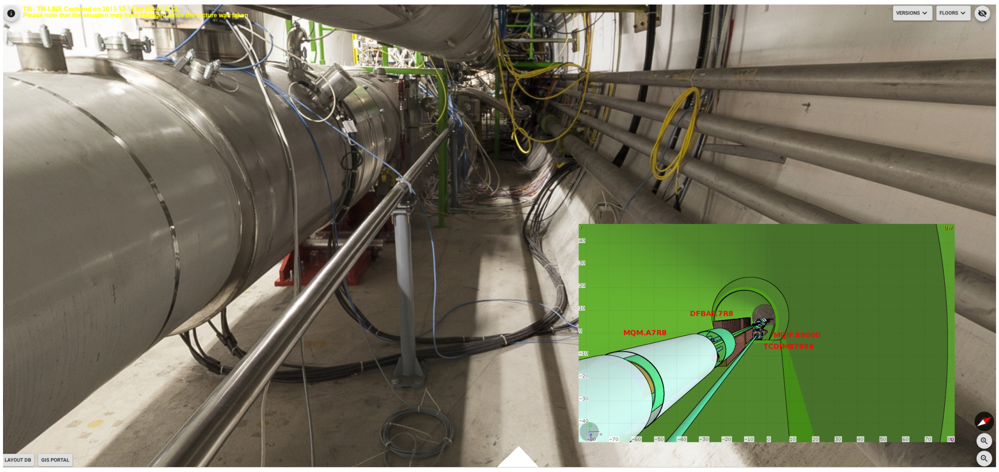

Figure 4: Comparison between FLUKA model and real tunnel around Q7 magnet. The model does not include jumper cables and additional service pipes.

a factor of 2 in the signal response.

The values of the calibration factors are reported in Table 1.

The percentage difference between simulated and measured signals is at most 41% except for the BLMI.87905 whose position was not verified during the site visit because of difficulty with access. For the vertical BLMIs, the agreement with the experimental values was improved after implementing a simplified model of the TCDI assembly, including the motors and the support (placed side-ward), which can attenuate the shower propagation toward the BLMI. The results in Table 1 refers to a TCDI model with two 3D box of about 23 kilograms made of a compound of aluminum and iron with an equivalent density of 1.7 g/cm^3. By assigning a double equivalent density to the motors, simulated signals decrease by about 10%. No LHC-BLM measurement data are available for comparison.

4.2 Loss map method

From the analysis of simulated input losses for horizontal oscillations (12 oscillation phases every 30°), the total amount of lost protons on the collimators are in the range 35% - 65% depending on the phase oscillation. The BLMI signals are dominated by the number of impacts on the upstream collimator. Therefore, the comparison with loss maps should be used to evaluate the reliability of the experimental condition (e.g. beam trajectory, steering effect). Expected losses per injection pulse were evaluated as:

$$p^{+}{}_{impacting}/p^{+}{}_{inj} = \frac{S_i^{\mathrm{BLMI}}[Gy]}{C_i[Gy/p^{+}{}_{impacting}]}\frac{1}{I[p^{+}{}_{inj}]} \tag{2}$$

where S_i^{BLMI} is the measured BLMI signal, (C_i) is the average of calibration factors of the right and left jaws (from Tab.1) expressed in Gy per lost proton, and I is the injected beam intensity.

The relative difference between the number of protons impacting on the collimator evaluated by MAD-X and estimated experimental BLM signal using the Eq. 2 is shown in Fig. 5

BLMI name	TCDI type	Measure (pGy/proton)	Simulation (pGy/proton)	Δ (%)
Left/Up jaw				
BLMI.87441	TCDIH	4.1	4.9	20
BLMI.87645	TCDIV	5.5	7.6	38
BLMI.87804	TCDIV	6.5	8.5	32
BLMI.87905*	TCDIH	6.4	8.5	34
BLMI.88122	TCDIH	2.3	2.2	-4
BLMI.88126	TCDIV	1.9	2.3	20
Right/Down jaw				
BLMI.87441	TCDIH	3.6	4.3	19
BLMI.87645	TCDIV	5.7	7.7	35
BLMI.87804	TCDIV	6.1	8.7	41
BLMI.87905*	TCDIH	5.6	8.9	57
BLMI.88122	TCDIH	2.4	2.5	5
BLMI.88126	TCDIV	2.0	2.3	12

* BLMI position not verified

Table 1: BLMI signal calibration results.

for each oscillation case. The figure includes only the collimator that are impacted by more than 0.1% of the simulated injected intensity. In most of cases, a remarkable difference is observed because the cross-talk due to the losses on an upstream collimator that might induce a signal in a downstream BLM and to a possible variation of the beam trajectory with respect to the ideal one (see Sec. 4.2.2).

Loss maps with variation larger than 50% are deemed not to describe realistically the experimental losses. For the convenience of this study, the oscillation phases are divided in two groups, each with a dedicated analysis procedure :

1. The nominal trajectory cases correspond to loss maps with a variation smaller than 50% with respect to the number of impacts predicted by the MAD-X simulation (see 4.2.1). For those oscillations, the results of the shower simulation is compared directly with the experimental response of the BLMs.

2. The off-nominal trajectory cases, instead, corresponds to the scenario with a large discrepancy. For a selected oscillation, a sensitivity analysis of the collimator gap center position was performed (see 4.2.2).

In both cases, the computed LHC-BLM signal is compared to the measured one.

4.2.1 Nominal trajectory case

For selected oscillations of the first group, the comparison between the BLMI simulated signals and the experimental data is showed in Fig. 6. It must be noted that the variation of experimental signals recorded during Run II (2016-2017-2018) is not negligible as showed

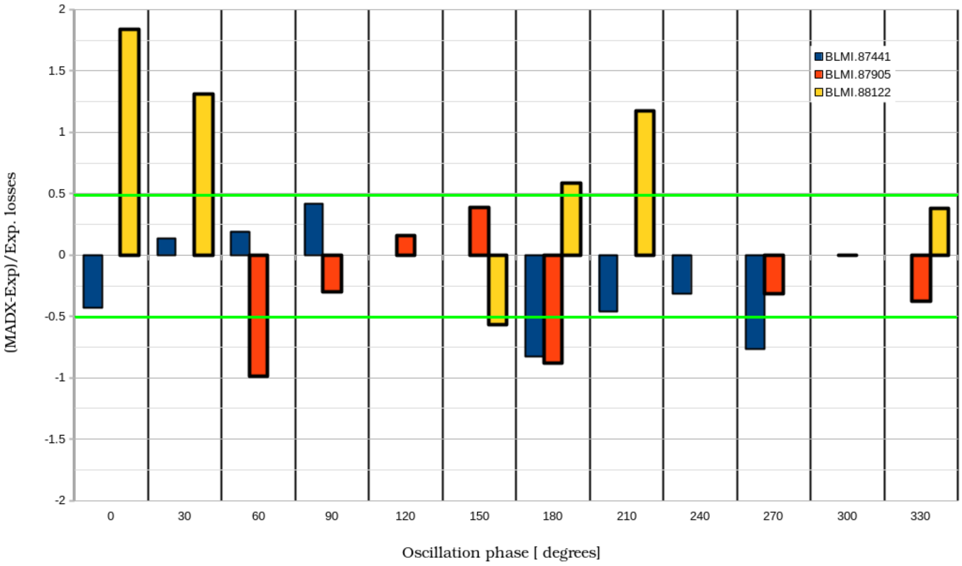

Figure 5: Variation between the number of impacts evaluated with MAD-X simulation and the ones estimated from measured signals using Eq. 2. Green lines represent variation of 50%.

with the grey band. In addition, the signal measured by some BLMIs is close to the smallest detectable signal, which is ~ 0.13 mGy.

As an example, the comparison with the LHC-BLM is shown in Fig. 7 for the 330° oscillation case. According to the MAD-X simulation, the number of impacting protons on the second horizontal collimator and on the third one are $\sim 20\%$ and $\sim 15\%$ of the total intensity, respectively. It is to note that the LHC-BLMs placed on B2-side display a signals higher than the ones placed on B1-side by an order of magnitude. Even with a 40% disagreement between measurements and source term, the simulated BLMI signal pattern fairly reproduce the experimental values: the difference between simulation and measurement is between 20% and 60%.

For the other oscillation phases of the nominal trajectory case group, the comparisons are reported in the Appendix (Fig. 15).

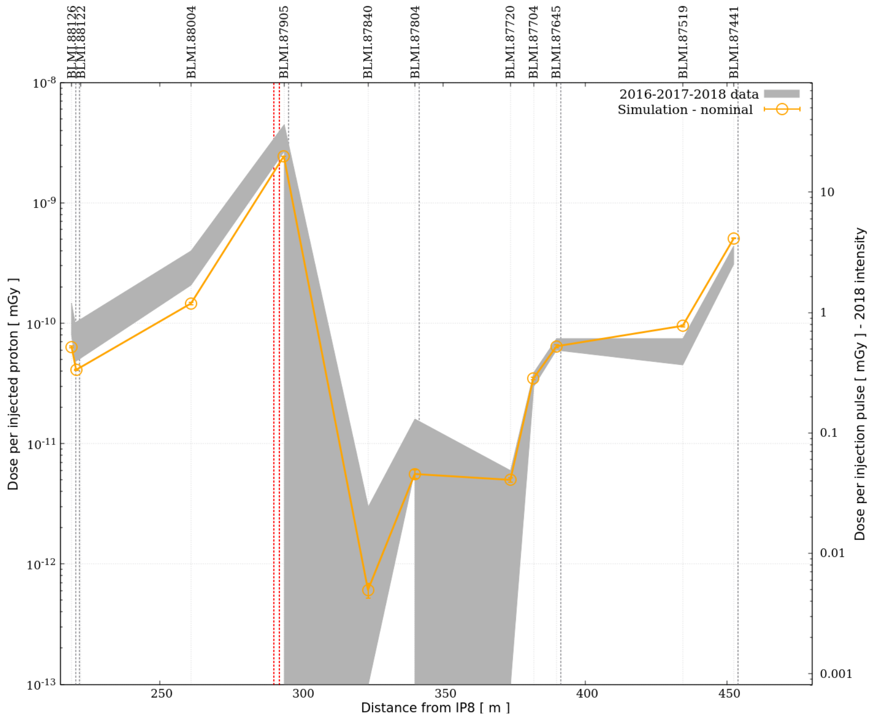

(a) 90°

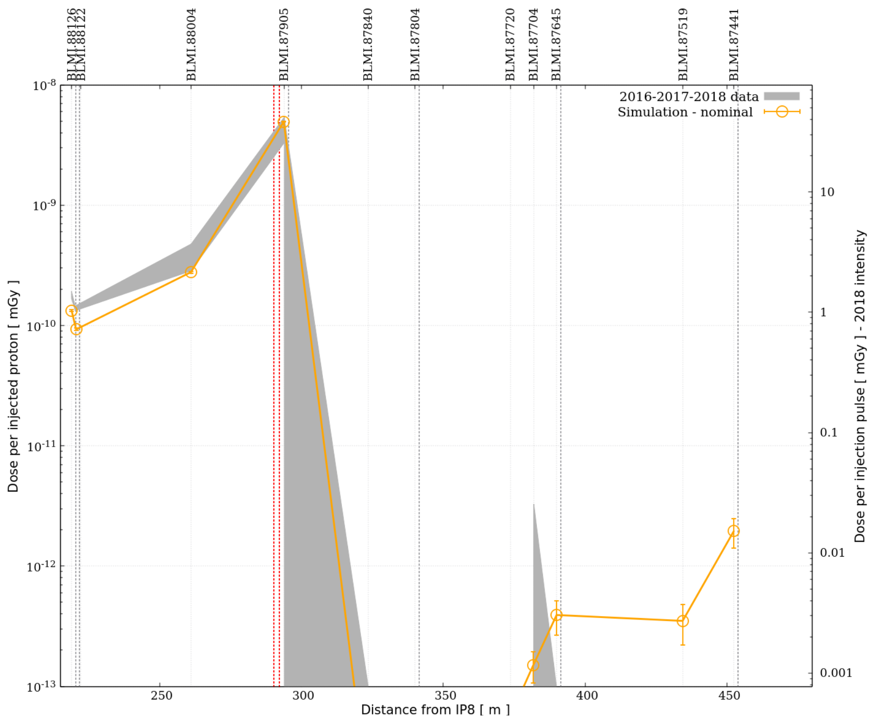

(b) 120°

Figure 6: BLMI signals induced by the beam horizontal oscillation phase of 90° (6a), 120° (6b). Comparison between simulation (in yellow) and experimental data (grey band). Dose is normalized to the number of injected protons to compare experimental data collected with different intensities. The vertical right axis reports dose per pulse considering 2018 intensity. The beam comes from the right. The red vertical lines indicate the position of the present iron shield and the grey ones the TCDIs.

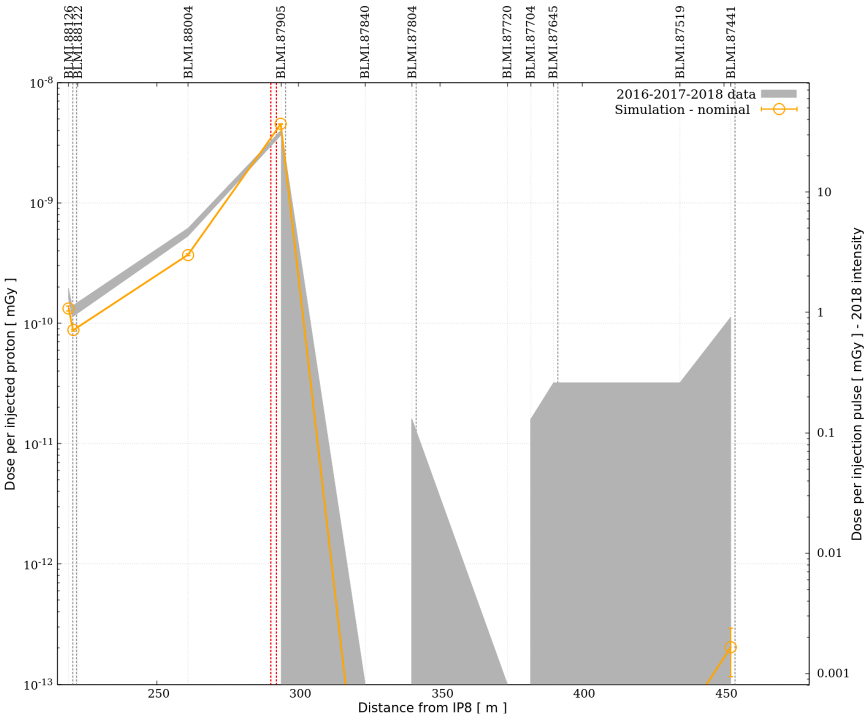

(c) 300°

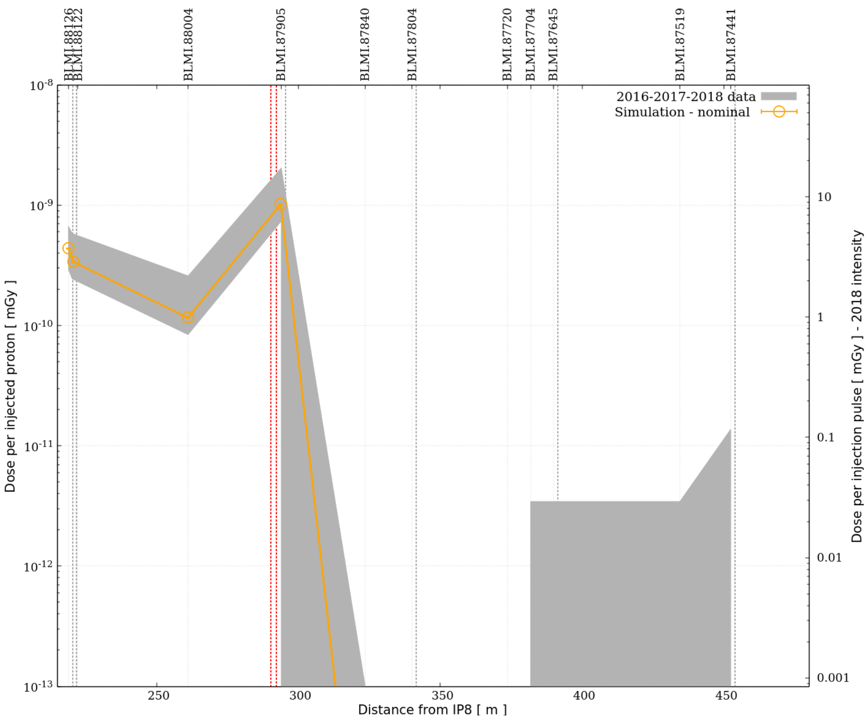

(d) 330°

Figure 6: BLMI signals induced by the beam horizontal oscillation phase of 300° (6c), 330° (6d). Comparison between simulation (in yellow) and experimental data (grey band). Dose is normalized to the number of injected protons to compare experimental data collected with different intensities. The vertical right axis reports dose per pulse considering 2018 intensity. The beam comes from the right. The red vertical lines indicate the position of the present iron shield and the grey ones the TCDIs.

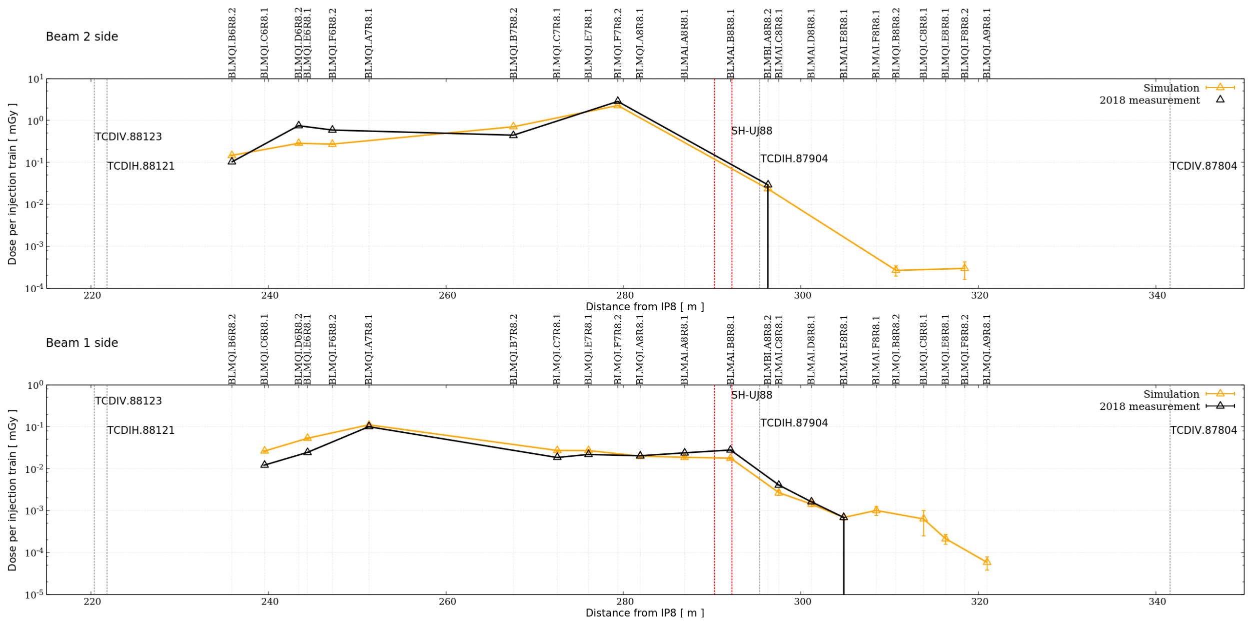

Figure 7: LHC-BLM signals induced by a beam horizontal oscillation phase of 330°. Simulation (in yellow) and experimental data (in black) are reported for B1-side (bottom) and for B2-side (top). The beam comes from the right. The red vertical lines indicate the position of the present iron shield and the grey ones the TCDIs.

4.2.2 Off-nominal case: sensitivity analysis

The loss maps, which are generated by the MAD-X tracking simulations assuming an ideal machine, cannot provide a realistic source term for most cases of Fig. 5. Taking the 60° phase oscillation as case study, MAD-X losses are mostly concentrated on the first collimator and only few protons arrive at the second horizontal collimator (TCDIH.87904). Using the 2018 experimental data and the simulated calibration factors (together with the Eq. 2), one can conclude that losses have a different sharing between the two most upstream horizontal collimators. The largest difference is for TCDIH.87904, for which the difference is about a factor of 50.

Starting from a full MAD-X distribution at the beginning of the model instead of a loss map, the FLUKA simulation provides consistent results with the MAD-X simulations in terms of primary protons on the collimators. The contribution of the elastically scattered protons from the first collimator increase the number of impacts on the second one but not enough to reproduce the experimental signals.

In both cases, the source distributions are generated assuming an ideal machine in MAD-X and do not include shot-to-shot trajectory variations which have to be expected since the orbit in the SPS is not always exactly the same and because of the ripples in the waveform of the extraction kickers and septa. For a typical beam size of 0.5 mm, the tolerance of transfer line collimators is $1.4\,\sigma$ [10]. To implement a set-up error in the Fluka model, a gap shift is applied (keeping the nominal aperture) in compliance with the tolerance estimation. The sensitivity analysis shows how different assumptions on the collimator set-up could influence the distribution of losses.

Tables 2 and 3 report the percentage of primary protons impinging on each horizontal collimator as a function of gap shift expressed in σ. The last column indicates the percentage of experimental impacts evaluated with Eq. 2. Therefore, it is important to consider that the experimental BLM signal include the cross-talk due to beam showering and to elastic interactions of protons scattered back into the beam pipe by the upstream collimators. For this reason, in Tables 2 and 3 the sum of the experimental losses is not reported. As showed in Table 2, the estimated gap adjustment of the first horizontal (TCDIH.87441) is smaller than 0.5 σ.

Collimator	Impacts TCDIH.87441 aperture				Measurements (Eq. 2)
	-	$0.5\,\sigma$	$1\,\sigma$	$1.4\,\sigma$	
TCDIH.87441	45.4%	27.8%	13.9%	0.5%	38.1%
TCDIH.87904	0.15%	0.29%	0.45%	0.79%	8.2%
TCDIH.88121	0.002%	0.004%	0.008%	0.025%	0.7%
Total	45.6%	28.1%	14.4%	1.3%	-

Table 2: Sensitivity analysis of impacts to the first TCDIH set-up. The sum of the experimental losses is not reported since it would includes the cross-talk from upstream collimators (see text for more details).

Collimator	Impacts TCDIH.87904 aperture				Measurements (Eq. 2)
	-	$-0.5\,\sigma$	$-1\,\sigma$	$-1.6\,\sigma$	
TCDIH.87441	45.4%	45.4%	45.4%	45.4%	38.1%
TCDIH.87904	0.15%	0.9%	3.8%	9.5%	8.2%
TCDIH.88121	0.002%	0.002%	0.002%	0.002%	0.7%
Total	45.6%	46.3%	49.2%	54.9%	-

Table 3: Sensitivity analysis of impacts to the second TCDIH set-up. The sum of the experimental losses is not reported since it would includes the cross-talk from upstream collimators (see text for more details).

Table 3 shows the sensitivity analysis varying the aperture shift of the second horizontal collimator so that one of the jaw intercepts more protons. The analysis of the impacts cannot be not exhaustive because it does not take into account the signal cross-talk due to the proton impacting on the upstream collimator. A full simulation shows that an aperture shift of the second horizontal collimator of $0.8 - 1\sigma$ can reproduce the experimental loss sharing. The comparison between BLMI simulated signals and data collected in 2016, 2017 and 2018 is showed in Fig. 8. Including the protons that interacted elastically with the first collimators, this gap shift range of TCDIH.87904 provides the most realistic loss amount on TCDIH.87904 and impact sharing between collimators.

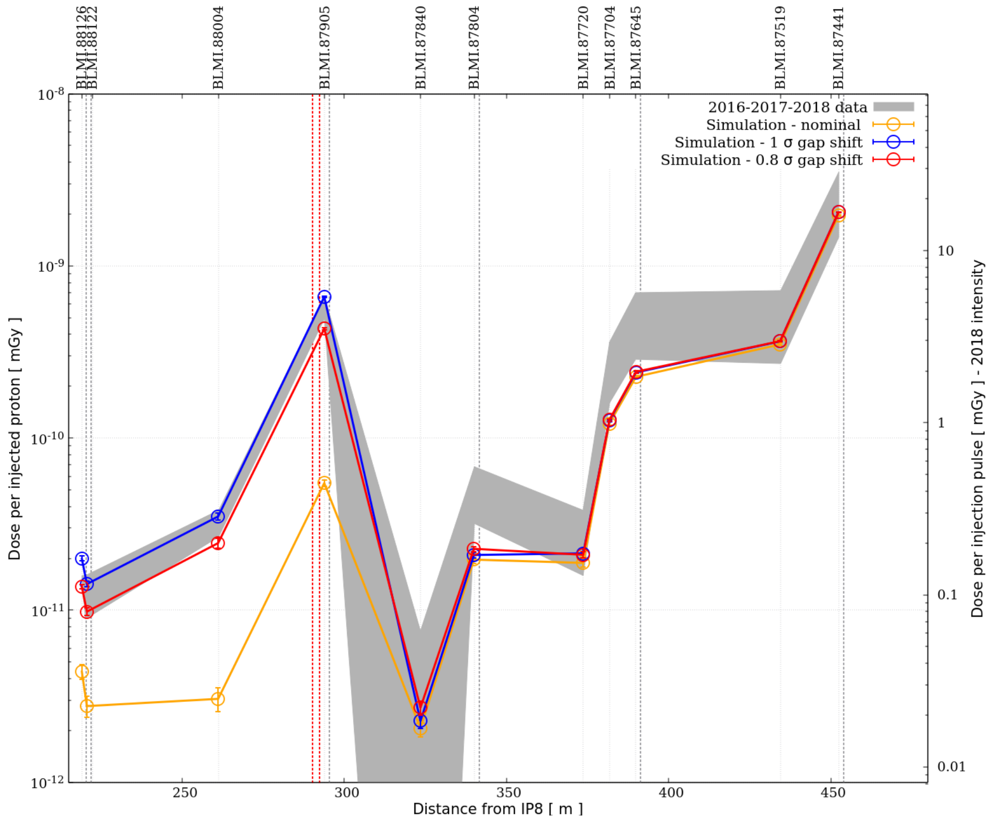

Figure 8: Results for BLMI signals induced by a beam horizontal oscillation phase of 60°. Comparison between simulated signals and experimental data (grey band). Simulation with nominal collimator apertures is in yellow and with TCDIH.87904 aperture shift of 0.8 σ in red and of 1 σ in blue. Dose is normalized to injected protons to compare experimental data collected with different intensities. Instead, the right y shows dose per pulse considering 2018 intensity. The beam comes from the right. The red vertical lines indicate the position of the present iron shield and the grey ones the TCDIs.

With the estimated shifts, the LHC-BLM simulated signals and the 2018 measurements show a quite good agreement (Fig. 9). The differences stem from the two main limitations of the model. The first is that loss maps were produced considering the ideal trajectory, while possible shot-to-shot variation may have occurred. The second is related to the geometrical implementation of the tunnel, in which some details of the cables and service pipes are not included from 270 to 290 metres from IP8 (see Section 3).

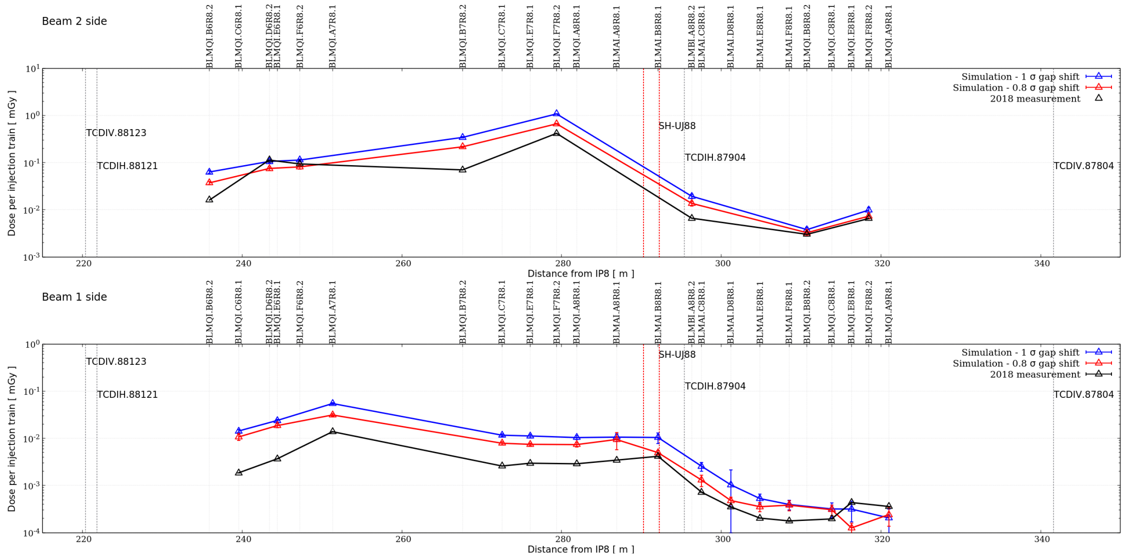

Figure 9: Results for LHC-BLM signals induced by a beam horizontal oscillation phase of 60° with shifted aperture of TCDIH.87904. Comparison between experimental data (in black), simulation with aperture shift of $0.8\,\sigma$ (in red) and of $1\,\sigma$ (in blue). Bottom and top plots show respectively B1-side and B2-side LHC-BLM signals. The beam comes from the right. The red vertical lines indicate the position of the present iron shield and the grey ones the TCDIs.

4.3 Application example: LHC dump event

An instructive example is the study of instability at flat top in the SPS that occurred on 17 May 2018 in Q7R8 and induced a beam dump. The instability affected the last ten bunches of the train before being extracted from SPS towards TI8 as showed in Fig. 10.

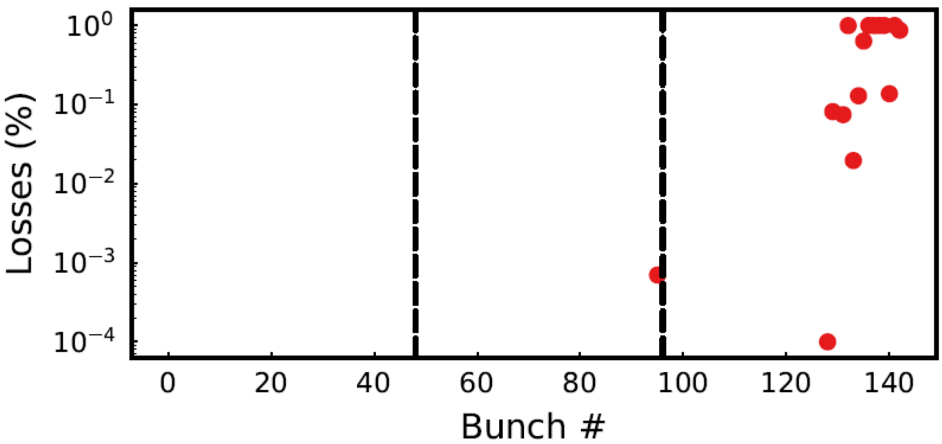

Figure 10: Bunch-by-bunch data registered by transfer line BPM during the injected train for LHC dump event of 17 May 2018. Losses are observed mainly at the end of the train.

The accident provides the possibility to test the model in a different experimental case.

4.3.1 Source term and method

The loss map was generated using the information of the Beam Position Monitor (BPM) measurements, so that the trajectories of each individual bunch have been reconstructed with MAD-X.

The injection train was made by 144 bunches, each with an intensity of $(1.13 \cdot 10^{11})$. The normalization for LHC-BLM induced signal was assumed to be $1 \cdot 10^{12}$ lost protons per injected train, corresponding to around 6.3% of the total pulse.

The losses are distributed on the horizontal collimators, mainly the first two (see Fig. 11). Protons hit both jaws of the first two collimators.

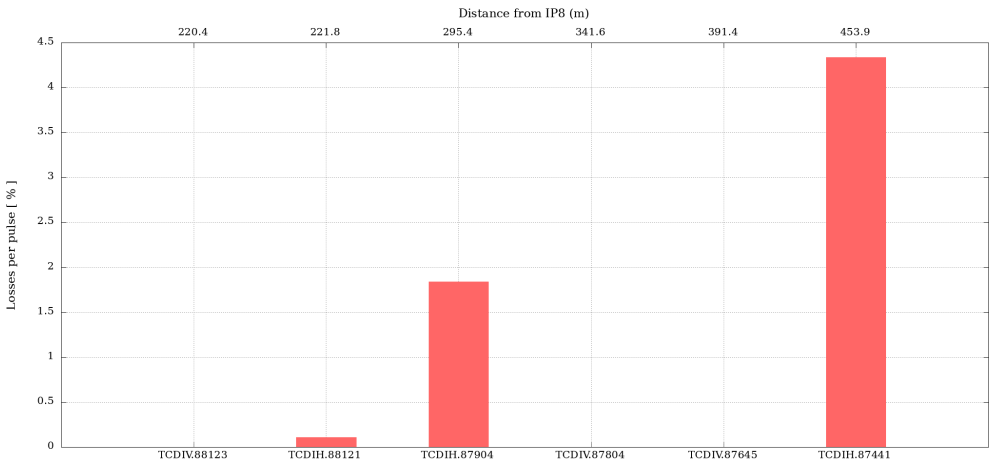

Figure 11: Loss distribution on collimators for Quench of May 2018 [14].

4.3.2 Results

During the LHC dump event, most of the detectors are saturated (over 23 Gy/s). For these BLMs the simulated signals are systematically higher than the measured ones consistently with the BLM electronic saturation limit. For the LHC-BLMs not saturated, the agreement obtained is very good (see Fig. 12). From the simulation it is possible to determine the energy density in the magnet coils. For the two most exposed magnets, a peak energy density of 4 mJ/cm^3 and 0.3 mJ/cm^3 has been estimated for the Q6 and Q7 magnet, respectively. Since the magnet quench limit for those magnets are in the range 30-40 mJ/cm^3 at the injection energy [15], it can be concluded that the dump event was not caused by the energy deposition in the coils. This result is in agreement with what is reported in the MP3 quench database, where the LHC dump event of 17 May 2018 has been classified as a beam loss induced trigger of a DQHDS (Quench Heater Discharge Power Supply) [16].

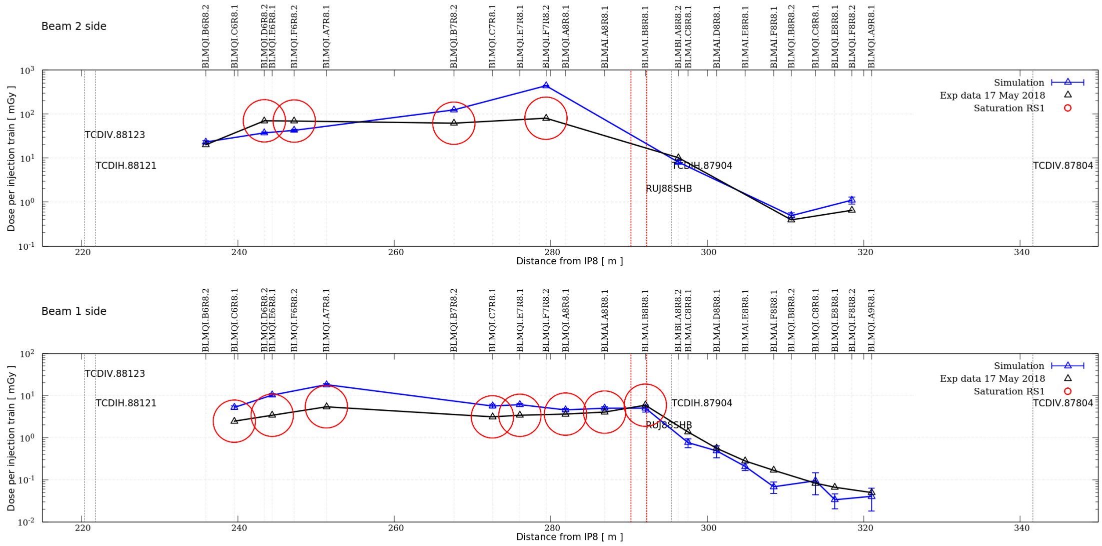

Figure 12: Comparison between LHC-BLM experimental signals (black) and simulated ones (blue) for Quench of May 2018. The red circles indicate the saturated BLMs. Bottom and top plots show, respectively, B1-side and B2-side LHC-BLM signals. The beam comes from the right. The red vertical lines indicate the position of the present iron shield and the grey ones the TCDIs.

5 Shielding simulation for the LIU scenario

LIU project aims at increasing the beam intensity in order to match the HL-LHC requirements. The upgrade of the transfer line collimator system is intended to attenuate the new beam intensity to safe levels in case of mis-injection. A new TCDI model (TCDIL) was designed considering the most severe conditions for the transfer line collimators. TCDILs are almost 1 meter longer than the current model, 2.1 m instead of 1.2 m [2]. Regular losses on the TCDIL collimators during the injection into LHC induce particle showers on the LHC-BLMs and, therefore, they can systematically trigger unnecessary beam dumps. Dedicated shields installed in the injection line can attenuate the signal of the most exposed BLMs, thus avoiding the need to blind these BLM's by during the injection process. While there are no significant modifications in the TI2 layout, the position of three collimator in TI8 is changed significantly, because of space constrains.

The TI8 geometry model adapted to the layout post-LS2 was used to study the effects of the operational injection losses on the LHC-BLM in the LIU configuration and evaluating a shielding solution able to reduce signals induced by injection losses.

5.1 Source term and method

In the LIU scenario, four beam loss cases were selected, each one corresponding to a different horizontal oscillation phase ($0° - 150° - 180° - 330°$ and $1.4\,\sigma$ amplitude). From operational experience, the losses in TI8 are mainly at the two first horizontal collimators. The loss maps were evaluated with TCDI apertures of $\pm 4.5\,\sigma$ with an emittance of $3.5\,\mu$m.

The beam parameters used for the LIU scenario are:

- Beam momentum: 450 GeV/c.
- HL-LHC intensity: $2.3 \cdot 10^{11} \cdot 288$ ppp
- Losses per HL-LHC train : $\sim 5 \cdot 10^{9}$ protons [17].

5.2 Results

Even without any shield, the B1-side LHC-BLM signals reach values lower than 0.1 mGy/pulse, which are below the dump threshold by more than a factor of 3. Some of the B2-side LHC-BLMs show signals above the dump threshold. The geometry of this region plays a significant role because the TI8 pipe gets very close to the LHC-BLMs and the LHC beamlines. A shielding system has been studied to limit the losses cross-talk from TL to LHC. The reduction on each LHC-BLM signal is mainly due to the closest upstream shield and the effect of each shield is independent from the other shields. For each relevant BLM, the design of the respective shield has been studied. The following iron shields have been studied:

1. Shielding block already installed (SH-UJ88).
2. L-shaped iron shield downstream the TCDILH.87939 (SH-RH87).
3. Shield for leakage placed as close as possible to the downstream LHC-BLM on Q6 cryostat (SH-RA87) at 250 m from IP8.

The effect of the different shields is compared with respect to the reference case where no shields are present in the TI8 line. The effectiveness of the proposed shields for each pair of oscillations ($0° - 180°$ and $150° - 330°$) are showed in Fig. 13. SH-RH87 decreases the BLMQI.B7R8 signal below the dump threshold for both cases. The current shielding in the SH-UJ88 further reduces signals below the dump threshold. SH-RA87 decreases the signals till a factor 4 down the dump threshold. On basis of the loss maps, the reduction factor changes between a factor $2 - 3$.

Optimized shielding geometries were studied to take into account the integration requirements, the space availability and shielding efficacy. The final shield configuration is showed in Fig. 14.

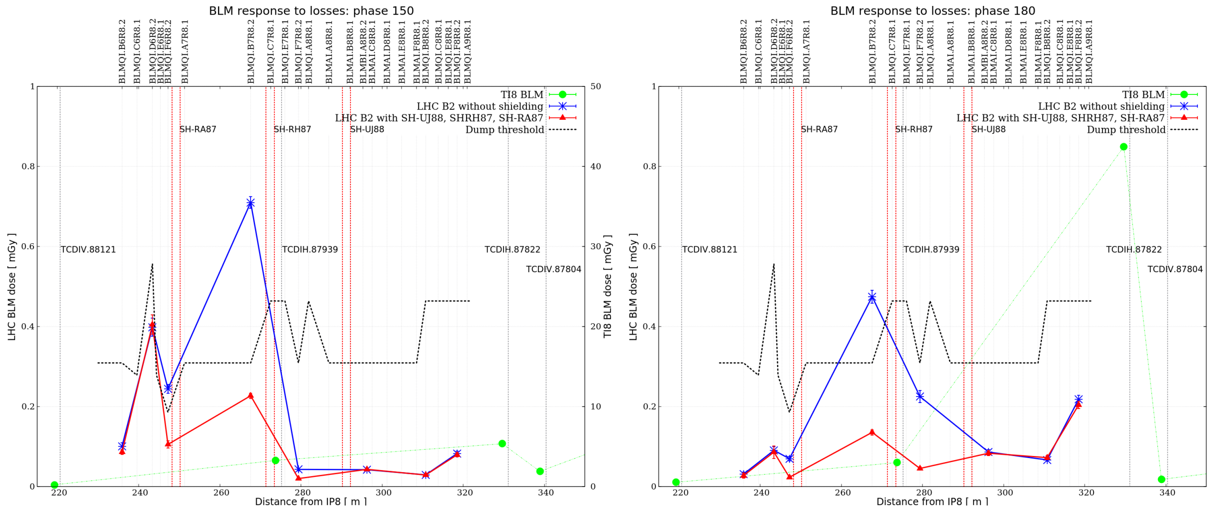

(a) 150°   (b) 180°

Figure 13: B2-side LHC-BLMs signals induced by a beam horizontal oscillation with phase equal to 150° and 180° (left and right plot, respectively) in absence (blue curves) and in presence (red curves) of the shielding system. The dashed black curve represents the threshold values for RS 01. The left axis refers B2-side LHC-BLMs signals while the right axis refers to the simulated BLMI signals (green dashed line)

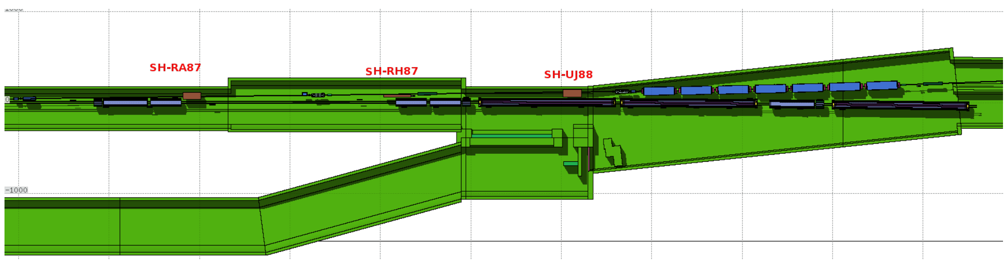

Figure 14: LIU geometry model with the shielding system to be installed.

6 Conclusion

A FLUKA model of the TI8/IR8 beamlines has been developed. The validation of the model has been performed against the BLM signals in controlled experimental losses scenarios. This study shows that the model is very sensitive to the loss maps. Although their accuracy is sufficient during the TCDI commissioning to verify the collimator aperture, the loss maps do not always describe sufficiently the experimental losses for the accuracy looked for by the FLUKA model. As they were produced assuming the ideal trajectory, the off-nominal cases display dramatic impact on specific BLMs. Moreover, details, such as cables and service pipes, which cannot be easily implemented in the geometry model, provide an additional systematic uncertainty for specific BLM locations.

The agreement of the simulations with experimental data collected during the BLMI calibration factor campaign ranges within 5% and 41% depending on initial loss map accuracy. For ideal loss maps at different oscillation phases, the discrepancy for BLMI signals is generally within a few tens of percent for the cases where the variation between the number of impacts evaluated with MAD-X simulation and the ones estimated by the experimental calibration factors is lower than 50%. A good agreement is observed for the corresponding B2 LHC-BLM patterns between model predictions and measured signals. Systematic differences were found up to a factor of 3 for region around Q7 magnet. For the case of the quench of 17 May 2018 in Q7R8, the source term has been optimized on experimental BPM data. In that case the agreement is within a few tens of percent for no saturated LHC-BLMs. The model has been updated to LIU scenario and used to study a shielding solution in order to reduce the LHC-BLM signals due to the losses in case of mis-injection and reduce the probability of unnecessary beam dump requests.

A Appendix

This appendix contains the comparison between 2018 experimental data and simulated signals for LHC-BLM,that are induced by the beam horizontal oscillation phase of 90° (Fig. 15a), 120° (Fig. 15b), 300° (Fig. 15c). These results refer to the nominal trajectory case (as discussed in paragraph 4.2.1).

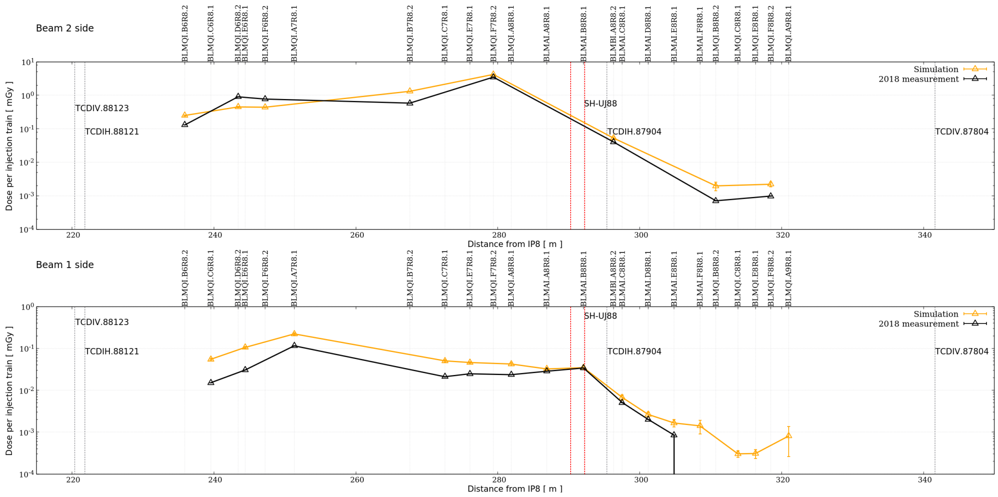

(a) 90°

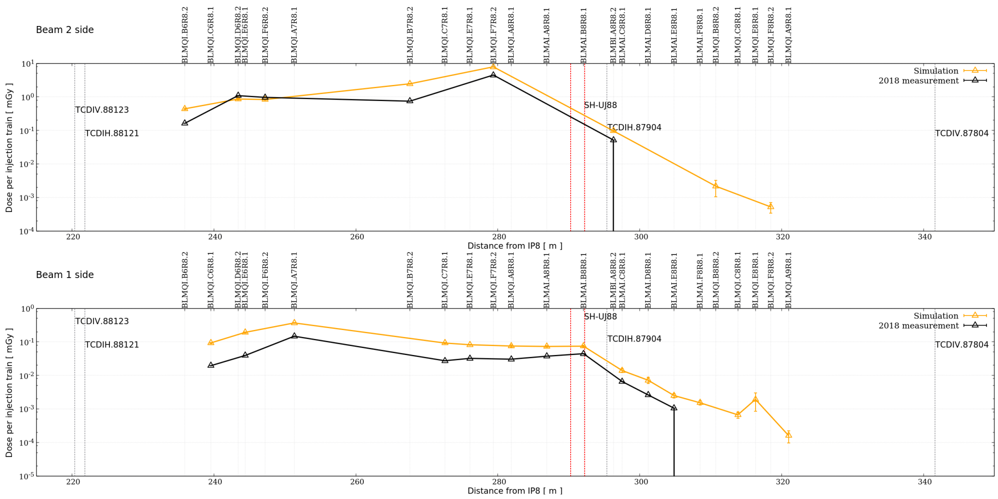

(b) 120°

Figure 15: Results for LHC-BLM signals induced by losses for different beam oscillation phases in the horizontal plane. Simulated signals due to ideal trajectory oscillations (in yellow) are compared to the experimental data.

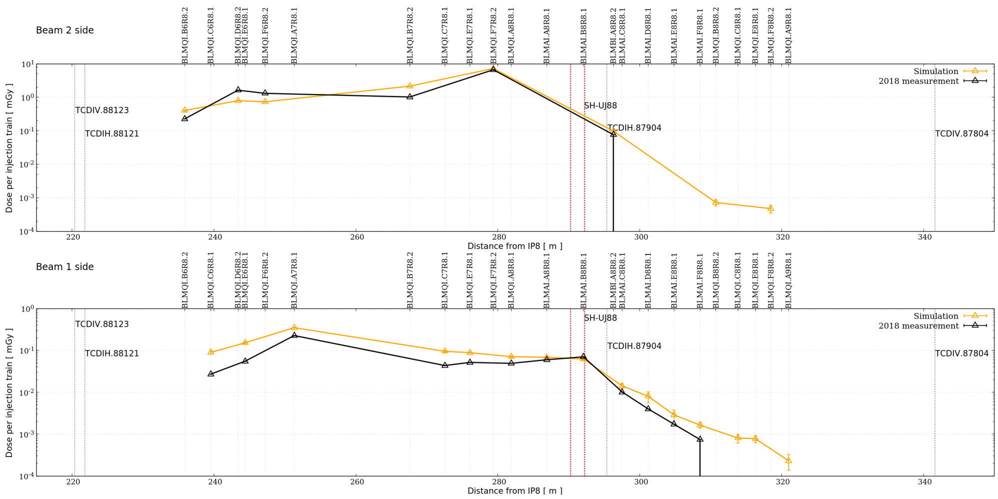

(c) 300°

Figure 15: Results for LHC-BLM signals induced by losses for different beam oscillation phases in the horizontal plane. Simulated signals due to ideal trajectory oscillations (in yellow) are compared to the experimental data.

References

[1] H. Damerau, A. Funken, R. Garoby, S. Gilardoni, B. Goddard, K. Hanke, A. Lombardi, D. Manglunki, M. Meddahi, B. Mikulec, G. Rumolo, E. Shaposhnikova, M. Vretenar, and J. Coupard. LHC Injectors Upgrade, Technical Design Report, Vol. I: Protons. Technical Report CERN-ACC-2014-0337, CERN, Dec 2014.

[2] M. A. Fraser. Functional and conceptual design of TCDI Transfer Line Collimators for LIU Upgrade. Technical Report LHC-TCDI-ES-0004, CERN, 2017.

[3] M. A. Fraser. Upgrade of the TCDI Collimators in the SPS to LHC Transfer Lines (TI2/TI8). Technical Report LHC-TCDI-EC-0002, CERN, 2019.

[4] V. Boccone. Update on the Shielding for the TI8 injection region. https://proj-lti.web.cern.ch/LTIcoordination/RelatedMeetings/LIBD/docs/LIBD_23-Nov-2011_boccone.pdf.

[5] V. Boccone, M. Brugger, and D. Kramer. Shielding for the TI8 injection region BLMs. https://indico.cern.ch/event/93338/contributions/1280065/.

[6] W. Bartmann, V. Boccone, C. Bracco, B. Goddard, V. Kain, and A. Nordt. TI8 shielding studies and angular alignment of TDI and TCDQ. http://cds.cern.ch/record/1351461, May 2011.

[7] BLM for SPS. https://wikis.cern.ch/display/BEBI/BLM+for+SPS.

[8] B. Dehning, E. Effinger, J. Emery, G. Ferioli, and C. Zamantzas. An FPGA Based Implementation for Real-Time Processing of the LHC Beam Loss Monitoring System's Data. (CERN-AB-2007-010), Nov 2006.

[9] E. B. Holzer, B. Dehning, E. Effinger, J. Emery, G. Ferioli, J. Gonzalez, E. Gschwendtner, G. Guaglio, M. Hodgson, D. Kramer, R. Leitner, L. Ponce, V. Prieto, M. Stockner, and C. Zamantzas. Beam loss monitoring system for the LHC. volume 2, pages 1052 – 1056, 11 2005.

[10] F.M. Velotti. *Higher brightness beams from the SPS for the HL-LHC era*. PhD thesis, Mar 2017. Presented 09 Mar 2017.

[11] T. T. Böhlen, F. Cerutti, M. P. W. Chin, A. Fassò, A. Ferrari, P. G. Ortega, A. Mairani, P. R. Sala, G. Smirnov, and V. Vlachoudis. The FLUKA Code: Developments and Challenges for High Energy and Medical Applications. *Nuclear Data Sheets*, 120:211–214, June 2014.

[12] G. Battistoni, T. Boehlen, F. Cerutti, P. W. Chin, L. S. Esposito, A. Fassò, A. Ferrari, A. Lechner, A. Empl, A. Mairani, A. Mereghetti, P. G. Ortega, J. Ranft, S. Roesler, P. Sala, V. Vlachoudis, and G. Smirnov. Overview of the FLUKA code. *Ann. Nucl. Energy*, 82:10–18. 9 p, 2015.

[13] A. Mereghetti, V. Boccone, F. Cerutti, R. Versaci, and V. Vlachoudis. The FLUKA LineBuilder and Element DataBase: Tools for Building Complex Models of Accelerator Beam Lines. *Conf. Proc.*, C1205201:2687–2689, 2012.

[14] F.M. Velotti. SPS-to-LHC TL TI8 tracking simulations of 17 May 2018 quench. https://edms.cern.ch/document/2286116/1, 26 July 2018.

[15] A. Apollonio and A. Verweij. Estimated Quench Levels for LHC High-Current Magnets, 2019.

[16] LHC Magnet Circuits, Powering and Performance Panel - MP3 Quench Database. https://twiki.cern.ch/twiki/bin/view/MP3/QuenchDatabase.

[17] F.M. Velotti and C. Bracco. LIU-TI8 expected nominal losses. https://indico.cern.ch/event/702596/, 7 February 2018.